Cell Reports, Volume *36*

Supplemental information

Immune mechanisms orchestrate tertiary lymphoid structures in tumors via cancer-associated fibroblasts

Anthony B. Rodriguez, J. David Peske, Amber N. Woods, Katie M. Leick, Ileana S. Mauldin, Max O. Meneveau, Samuel J. Young, Robin S. Lindsay, Marit M. Melssen, Salwador Cyranowski, Geoffrey Parriott, Mark R. Conaway, Yang-Xin Fu, Craig L. Slingluff Jr., and Victor H. Engelhard

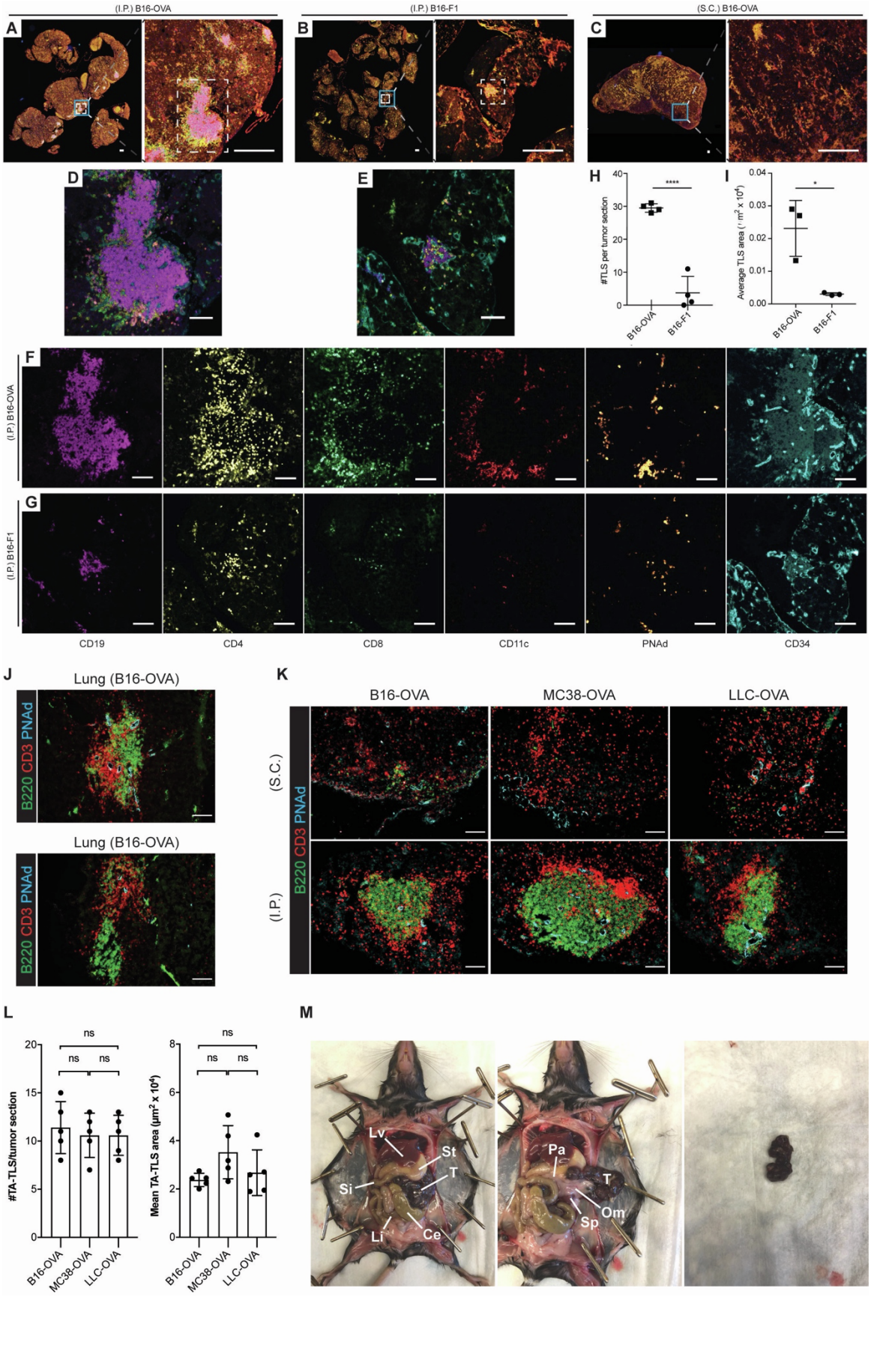
(I.P.) B16-OVA
(I.P.) B16-F1
(S.C.) B16-OVA
A
B
C
D
E
H
I
#TLS per tumor section
Average TLS area (/ mm² x 10⁴)
****
*
B16-OVA
B16-F1
F
G
(I.P.) B16-OVA
(I.P.) B16-F1
CD19
CD4
CD8
CD11c
PNAd
CD34
J
Lung (B16-OVA)
B220 CD3 PNAd
Lung (B16-OVA)
B220 CD3 PNAd
K
B16-OVA
MC38-OVA
LLC-OVA
(S.C.)
(I.P.)
B220 CD3 PNAd
L
#TA-TLS/tumor section
Mean TA-TLS area (µm² x 10⁴)
ns
B16-OVA
MC38-OVA
LLC-OVA
M
Lv
St
T
Si
Li
Ce
Pa
T
Sp
Om

Supplementary Figure S1: TA-TLS spontaneous develop in I.P. tumors and tumor-bearing lungs, but not S.C. tumors. Supplementary Figure S1 is related to Figure 1. C57BL/6 (WT) mice were S.C., I.P. or I.V. injected with B16-OVA, MC38-OVA, or LLC-OVA cells, as indicated. S.C. and I.P. tumors were harvested 14 days after implantation and lungs were harvested 21 days after I.V. injection. Preparation for imaging is described in Methods.
(A-C) Representative uncompensated multispectral image of S.C. and I.P. B16-OVA and B16-F1 tumors.
(D-G) Representative compensated multispectral images of TA-TLS in B16-OVA and B16-F1 I.P. tumors stained with indicated antibodies.
(H-I) Quantitative image summary data of TA-TLS in in B16-OVA and B16-F1 I.P. tumors. Data from 1 experiment (n=3-4 per group).
(J) Representative images of tumor-bearing lungs stained with indicated antibodies.
(K) Representative images of S.C. and I.P. tumors stained with indicated antibodies.
(L) Quantitative image summary data of TA-TLS in indicated I.P. tumors. Data from 1 experiment (n=5 per group).
(M) Representative images of an I.P. tumor situated in and resected from the peritoneal cavity. T, tumor; Lv, liver; St, stomach; Si, small intestines; Li, large intestines; Ce, cecum; Pa, pancreas; Om, omentum; Sp, spleen. Scale bars = 100 μm. Results shown as mean ± SD analyzed using unpaired Welch's t-test (H and I) or Kruskal-Wallis h-test with Dunn's post-test (L). ns: $p>0.05$, *$p<0.05$, **$p<0.01$, ***$p<0.001$, and ****$p<0.0001$.

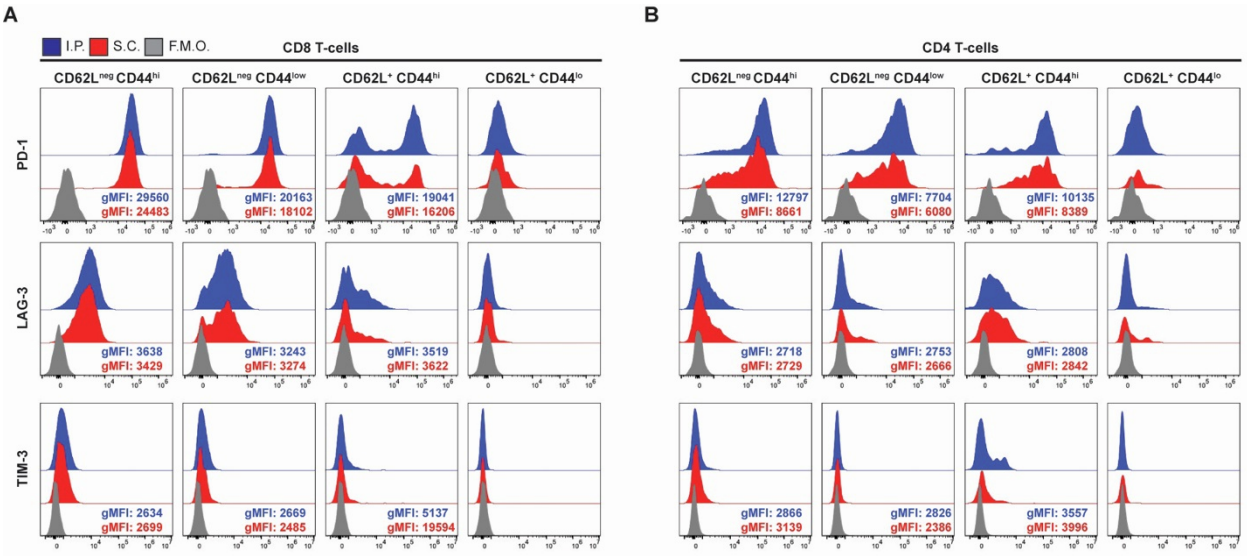

Supplementary Figure S2: S.C. and I.P. tumors contain distinctly differentiated T-cell populations. Supplementary Figure S2 is related to Figure 1. WT mice were S.C. and I.P. injected with B16-OVA cells. Tumors were harvested 14 days after implantation and analyzed by flow cytometry as described in Methods. Representative histogram plots and geometric mean fluorescence intensity (gMFI) of indicated markers on effector ($CD62L^{neg}$ $CD44^{hi}$), activated ($CD62L^{neg}$ $CD44^{lo}$), central memory ($CD62L^{+}$ $CD44^{hi}$), and naïve ($CD62L^{+}$ $CD44^{lo}$) T-cells from S.C. and I.P tumors. Data representative of 2 independent experiments (n=10 per group).

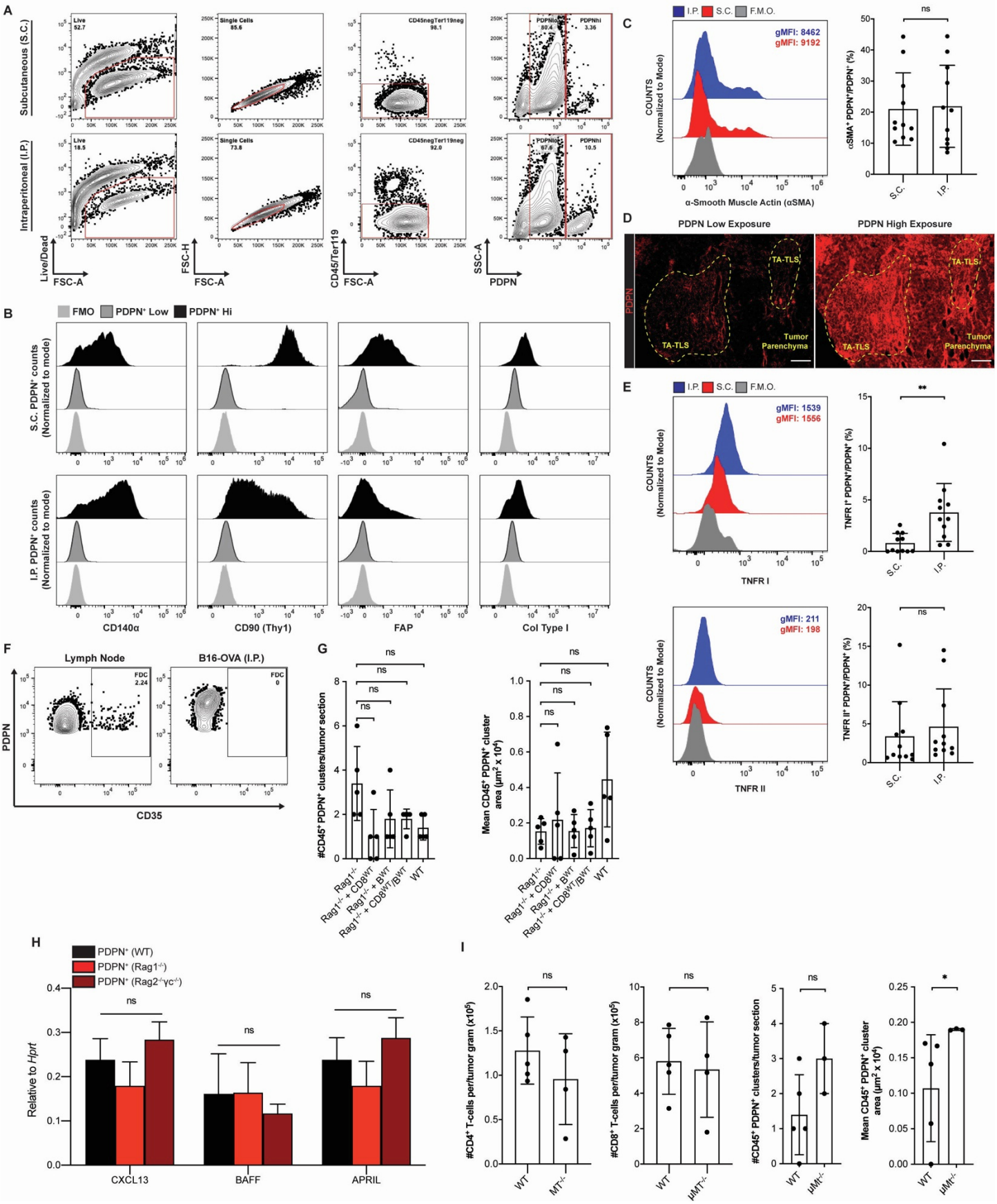
A
Subcutaneous (S.C.)
Intraperitoneal (I.P.)
Live
52.7
Live
18.5
Single Cells
85.6
Single Cells
73.8
CD45negTer119neg
98.1
CD45negTer119neg
92.0
PDPNlo
80.4
PDPNhi
3.36
PDPNlo
87.6
PDPNhi
10.5
Live/Dead
FSC-A
FSC-H
FSC-A
CD45/Ter119
FSC-A
SSC-A
PDPN
B
FMO
PDPN+ Low
PDPN+ Hi
S.C. PDPN+ counts (Normalized to mode)
I.P. PDPN+ counts (Normalized to mode)
CD140α
CD90 (Thy1)
FAP
Col Type I
C
I.P.
S.C.
F.M.O.
gMFI: 8462
gMFI: 9192
COUNTS (Normalized to Mode)
α-Smooth Muscle Actin (αSMA)
αSMA+ PDPN+/PDPN+ (%)
ns
S.C.
I.P.
D
PDPN Low Exposure
PDPN High Exposure
PDPN
TA-TLS
Tumor Parenchyma
E
I.P.
S.C.
F.M.O.
gMFI: 1539
gMFI: 1556
COUNTS (Normalized to Mode)
TNFR I
TNFR I+ PDPN+/PDPN+ (%)
**
gMFI: 211
gMFI: 198
TNFR II
TNFR II+ PDPN+/PDPN+ (%)
ns
F
Lymph Node
B16-OVA (I.P.)
FDC
2.24
FDC
0
PDPN
CD35
G
#CD45+ PDPN+ clusters/tumor section
Mean CD45+ PDPN+ cluster area (μm2 x 10³)
ns
Rag1-/-
Rag1-/- + CD8WT
Rag1-/- + βWT
Rag1-/- + CD8WT/βWT
WT
H
PDPN+ (WT)
PDPN+ (Rag1-/-)
PDPN+ (Rag2-/-γc-/-)
Relative to Hprt
CXCL13
BAFF
APRIL
ns
I
#CD4+ T-cells per/tumor gram (x10⁵)
#CD8+ T-cells per/tumor gram (x10⁵)
#CD45+ PDPN+ clusters/tumor section
Mean CD45+ PDPN+ cluster area (μm2 x 10³)
WT
MT-/-
μMT-/-
*
ns

Supplementary Figure S3: Characteristics of cancer-associated fibroblasts. Supplementary Figure S3 is related to Figure 2 and 4.

WT, Rag1$^{-/-}$, Rag2$^{-/-}\gamma c^{-/-}$ or µMT$^{-/-}$ mice were injected S.C. or I.P. with B16-OVA cells and tumors were harvested 14 days after implantation. (A-C, E-F, H) Tumors were analyzed by flow cytometry as described in Methods. (D) WT I.P. tumors were analyzed by IF as described in Methods. (G) CAF purified from tumors growing in WT, Rag1$^{-/-}$, and Rag2$^{-/-}\gamma c^{-/-}$ mice were analyzed by qPCR as described in Methods.

(A) Representative flow cytometry plots and gating strategy for the identification of PDPN^{lo} and PDPN^{hi} cells in CD45^{+} depleted S.C. and I.P. tumor suspensions from WT mice.

(B) Representative histogram plots for indicated markers on PDPN^{lo} and PDPN^{hi} cells from CD45^{+} depleted S.C. and I.P. tumor suspensions from WT mice.

(C) Left, Representative histogram plots and gMFI of αSMA in CAF from S.C. and I.P. tumors from WT mice. Right, summary data of the percentage of CAF expressing αSMA from WT S.C. and I.P tumors Data from 3 independent experiments (n=11 per group).

(D) Representative immunofluorescence images of an I.P. tumor from WT mice stained for PDPN at different exposure times.

(E) Left, Representative histogram plots and gMFI of indicated markers on CAF from S.C. and I.P. tumors from WT mice. Right, summary data of the percentage of CAF expressing indicated markers in WT S.C. and I.P tumors Data from 3 independent experiments (n=11 per group).

(F) Representative flow cytometry plot of CD35 expression on CD31^{neg} PDPN^{hi} CAF from WT LN and I.P. tumor suspensions.

(G) Summary data for loosely organized CD45^{+}/PDPN^{+} clusters in indicated tumors. Data from 1 experiment (n=3-5 tumor sections per group).

(H) Expression of *Cxcl13, TNFSF13B* (BAFF), and *TNFS13* (APRIL) in CAF from indicated I.P. tumors. Data presented as $2^{-\Delta CT}$ relative to *Hprt*. Data from 1 experiment (n=3-5 tumors per group).

(I) Left, summary data of the number of T-cells. Right, quantitative image summary data of the CD45^{+}/PDPN^{+} cluster number and size. Data represents 1 experiment (n=4-5 tumors per group).

Scale bars = 100 µm. Results shown as mean ± SD analyzed by unpaired Welch's t-test (D-F and I) or Kruskal-Wallis h-test with Dunn's post-test (H). ns: p>0.05, *P<0.05, **p<0.01, ***p<0.001, and ****p<0.0001.

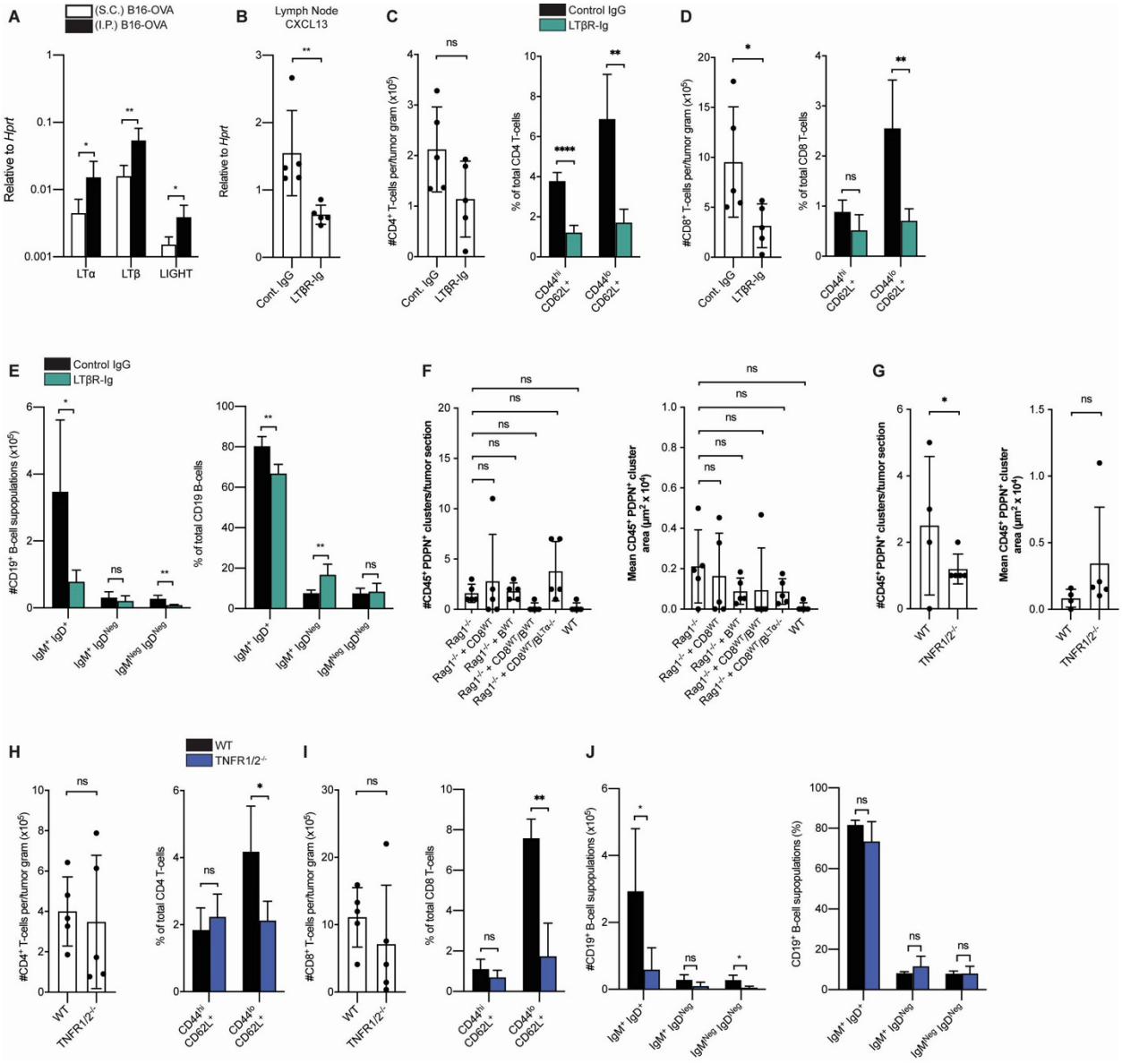

Supplementary Figure S4: LTβR and TNFR signaling influences the representation of naïve T- and B-cell in I.P. tumors. Supplementary Figure S4 is related to Figure 5.

WT or TNFR1/2$^{-/-}$ mice were S.C. or I.P. injected with B16-OVA cells, and tumors were harvested 14 days after implantation. In some cases (B-E), I.P. tumor-bearing mice were treated with a LTβR-Ig fusion protein. (A-B) whole tumor masses and inguinal LNs from tumor-bearing mice were analyzed by qPCR as described in Methods. (C-H) I.P. tumors were analyzed by flow cytometry as described in Methods.

(A) Expression of *Tnfsf1* (Ltα), *Tnfsf3* (LTβ), and *Tnfsf14* (LIGHT) in whole S.C. and I.P. tumors. Data represents 1 experiment (n=5 per group).

(B) Expression of *Cxcl13* in tumor-reactive lymph node from mice treated with control IgG or LTβR-Ig. Data presented as $2^{-\Delta CT}$ relative to *Hprt*. Data represents 1 experiment (n=5 per group).

(C-D) Summary data of the total number of T-cells, and percentage of T-cells that are central memory (CD62L^{+} CD44^{hi}) and naïve (CD62L^{+} CD44^{lo}). Data represents 1 experiment (n=5 per group).

(E) Summary data of the percentage of B-cells that are naïve (IgM^{+} IgD^{+}), memory (IgM^{+} IgD^{neg}), and class-switched (IgM^{neg} IgD^{neg}). Data represents 1 experiment (n=5 per group).

(F-G) Summary data for CD45^{+}/PDPN^{+} clusters in indicated tumors. Data represents 1 experiment for each panel (n=4-5 tumors per group).

(H-I) Summary data of the total number of T-cells, and percentage of T-cells that are central memory ($CD62L^+$ $CD44^{hi}$) and naïve ($CD62L^+$ $CD44^{lo}$). Data represents 1 experiment (n=5 per group).
(J) Summary data of the percentage of B-cells that are naïve (IgM^+ IgD^+), memory (IgM^+ IgD^{neg}), and class-switched (IgM^{neg} IgD^{neg}). Data represents 1 experiment (n=5 per group).
Results shown as mean ± SD. (A-H) Unpaired Welch's t-test. ns: $p>0.05$, *$p<0.05$, **$p<0.01$, ***$p<0.001$, and ****$p<0.0001$.

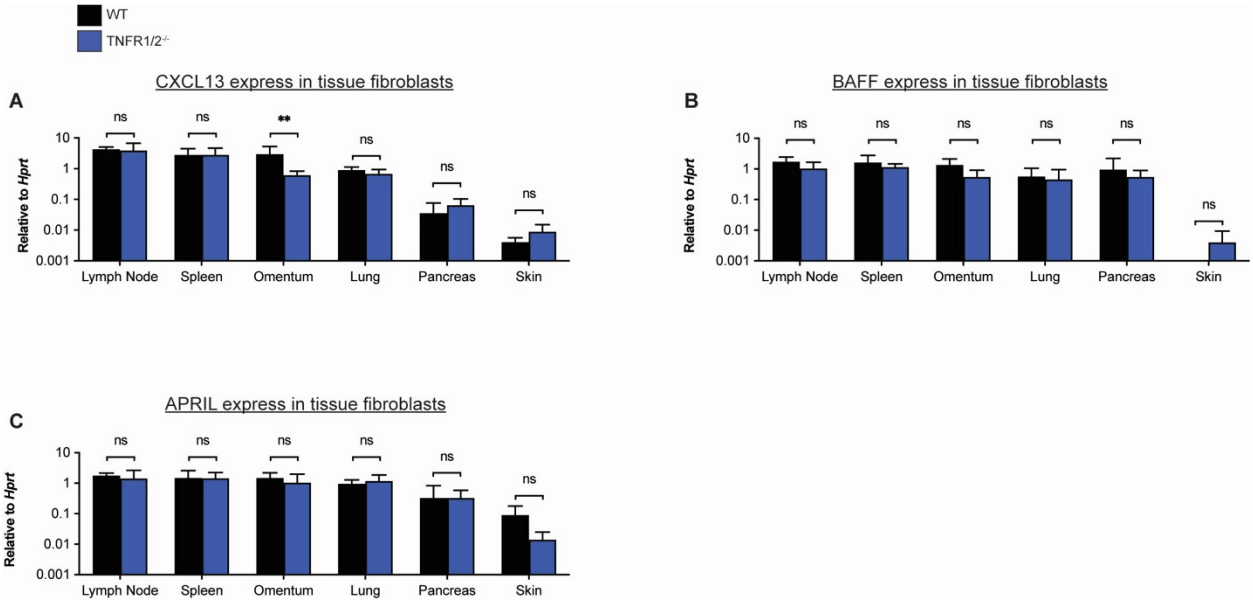

Supplementary Figure S5: CXCL13 expression, but not BAFF and APRIL, in omental fibroblasts is regulated by tumor necrosis factor receptor signaling. Supplementary Figure S5 is related to Figure 5. Tissue resident fibroblasts from indicated tissues of non-tumor bearing WT and TNFR1/2$^{-/-}$ mice were analyzed by qPCR as described in Methods.

(A-C) Expression of *Cxcl13, TNFSF13B* (BAFF), and *TNFS13* (APRIL) in fibroblasts from indicated tissues. Data presented as $2^{-\Delta CT}$ relative to *Hprt*. Data represents 1 experiment (n= 5 per group).

Results shown as mean ± SD. (A-C) Unpaired Welch's t-test. ns: $p>0.05$, *$P<0.05$, **$p<0.01$, ***$p<0.001$, and ****$p<0.0001$.

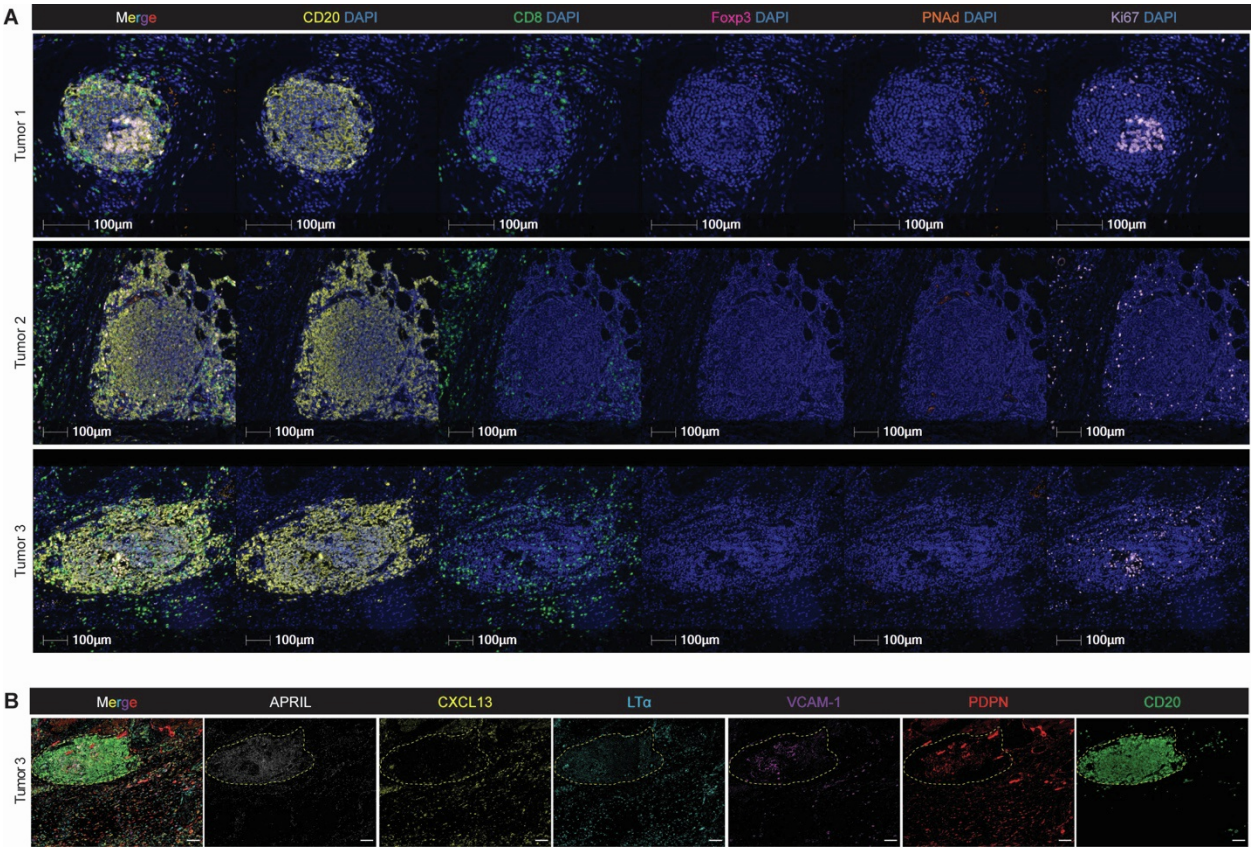

Supplementary Figure S6: TA-TLS in human melanoma contain similar cellular and molecular markers found in murine TA-TLS. Supplementary Figure S6 is related to Figure 6.
Human melanoma biopsies containing TA-TLS were collected, prepared, stained, and analyzed by multispectral imaging as described in Methods.
(A) Representative multispectral images of three independent human melanoma biopsies stained for indicated markers.
(B) Representative multispectral images of human melanoma biopsy #1 stained for indicated markers. Dashed region of interest represents TA-TLS area.
Scale bar = 100 µm.

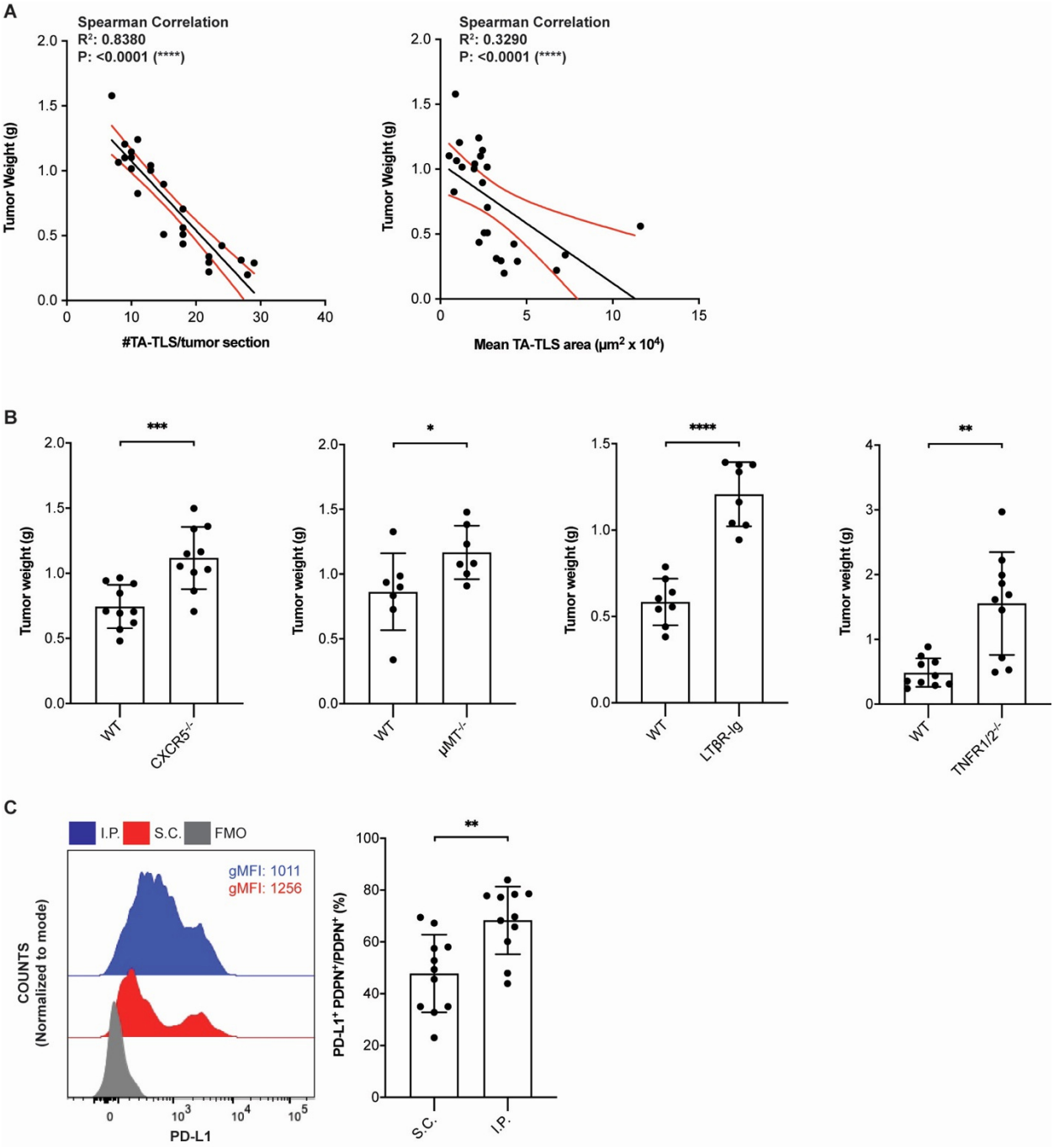

Supplementary Figure 7: I.P. tumors grown in knockout and LTβR-Ig treated mice are larger than those grown in WT mice. Supplementary Figure S7 is related to Figure 7.

WT, knockout, LTβR-Ig treated mice were S.C. or I.P. injected with B16-OVA cells and harvested on 14 days after implantation. (A-B) Tumors were harvest and weighed. (C) S.C. and I.P. tumors were analyzed by flow cytometry as described in Methods.

(A) Correlation analysis between the number and size of TA-TLS per tumor section against tumor weight. Red lines represent 95% confident intervals. Each point represents an individual I.P. tumor. Data represents five independent experiments (n= 25 I.P. tumors).

(B) Tumor weight of day 14 I.P. tumors grown in indicated mouse models. Data represents two-three independent experiments (n=8-10 per group).

(C) Representative histogram plots and gMFI of PD-L1 on CAF from S.C. and I.P. tumors from WT mice. Right, summary data of the percentage of CAF expressing PD-L1 from WT S.C. and I.P tumors. Data represents two independent experiments (n=11 per group).

Results shown as mean ± SD. (A) Spearman correlation analysis and (B-C) Unpaired Welch's t-test. ns: $p>0.05$, *$P<0.05$, **$p<0.01$, ***$p<0.001$, and ****$p<0.0001$.